Stable DNA Triple Helix Formation Using Oligonucleotides Containing 2′-Aminoethoxy,5-propargylamino-U†

Matthieu Sollogoub,[‡,⊥] Richard A. J. Darby,[§,#] Bernard Cuenoud,[∥] Tom Brown,[‡] and Keith R. Fox*[,§]

Department of Chemistry, University of Southampton, Highfield, Southampton SO17 1BJ, United Kingdom, and Division of Biochemistry & Molecular Biology, School of Biological Sciences, University of Southampton, Bassett Crescent East, Southampton SO16 7PX, United Kingdom, and Respiratory Diseases, Novartis Horsham Research Centre, Wimblehurst Road, Horsham, West Sussex RH12 5AB, United Kingdom

Received February 25, 2002; Revised Manuscript Received April 8, 2002

ABSTRACT: We have prepared oligonucleotides containing the novel base analogue 2′-aminoethoxy,5-propargylamino-U in place of thymidine and examined their ability to form intermolecular and intramolecular triple helices by DNase I footprinting and thermal melting studies. The results were compared with those for oligonucleotides containing 5-propargylamino-dU and 2′-aminoethoxy-T. We find that the bis-substituted derivative produces a large increase in triplex stability, much greater than that produced by either of the monosubstituted analogues, which are roughly equipotent with each other. Intermolecular triplexes with 9-mer oligonucleotides containing three or four base modifications generate footprints at submicromolar concentrations even at pH 7.5, in contrast to the unmodified oligonucleotide, which failed to produce a footprint at pH 5.0, even at 30 μM. UV- and fluorescence melting studies with intramolecular triplexes confirmed that the bis-modified base produces a much greater increase in T_m than either modification alone.

Intermolecular DNA triple helix formation provides a means for selectively targeting unique DNA sequences, which in principle may be useful for treating a wide range of diseases including cancer and viral infections (*1*−*9*). In this strategy, the DNA sequence of interest is targeted with a synthetic oligonucleotide, which binds in the major groove, making specific hydrogen bond contacts with exposed groups on the DNA bases (usually the purines) (*1*, *9*). Nucleic acid triple helices can be divided into two main classes, which differ in the orientation of the third strand oligonucleotide relative to the purine strand of the target duplex. Triplexes in which the third strand runs parallel to the purine strand are characterized by T·AT and C^+·GC triplets (*10*), while antiparallel triplexes consist of G·GC and either A·AT or T·AT triplets (*11*). Several other weaker triplets have also been described for recognition of pyrimidine bases, and a large number of nucleotide analogues have been prepared for extending the recognition code, and for generating complexes that are stable under physiological conditions (*12*).

One major limitation of the triplex strategy is that, although the complexes form with high specificity, the strength of binding is not as strong as that of the underlying duplex. Several strategies have been explored for increasing the binding affinity of the third strand. These include addition of ligands that bind to triplex (not duplex) DNA (*13*, *14*), covalent attachment of a DNA binding agent (usually an intercalator) which acts as a nonspecific anchor (*15*−*17*), addition of polyamines to the end of the oligonucleotide (*18*), the sugars (*19*), or the bases (*20*, *21*), modification of the phosphodiester backbone (*22*−*24*), and the design of novel bases with improved base stacking (*25*−*27*).

Although the T·AT triplet forms in a pH-independent fashion, several studies have shown that it has a lower stability than isolated C^+·GC triplets (*28*−*30*), presumably because the positive charge on the latter makes favorable interactions when stacked against the π-electrons of the adjacent triplets. We have used footprinting studies to examine the interaction of 9-mer oligonucleotides with oligopurine targets and have shown that, although TCCTTCTCT forms a stable triplex with a submicromolar dissociation constant, TTTTTTCTT does not generate a footprint even at concentrations as high as 30 μM (*30*). We have previously shown that addition of a positively charged group at the 5-position of thymine enhances the stability of the T·AT triplet (*31*, *32*). For these studies, we used 5-propargylamino-dU (U^P,[1] Figure 1A) as a charged thymine analogue. This analogue combines the benefits of the additional positive charge with the stacking of adjacent propyne moieties as previously observed with propynyl-dU (*33*, *34*). Although adjacent C^+·GC triplets have a destabilizing effect on triplex formation, third strands that contain

† This work was supported by grants from Cancer Research UK.

* Corresponding author: Prof. Keith R. Fox, Division of Biochemistry & Molecular Biology, School of Biological Sciences, University of Southampton, Bassett Crescent East, Southampton SO16 7PX, U.K., Tel. +44 23 8059 4374, Fax. +44 23 8059 4459, E-mail: krf1@soton.ac.uk.

‡ Department of Chemistry, University of Southampton.

§ Division of Biochemistry & Molecular Biology, School of Biological Sciences, University of Southampton.

∥ Novartis Horsham Research Centre.

⊥ Present address: Département de Chimie, Ecole Normale Supérieure, 24, rue Lhomond, 75231 Paris Cédex 05, France.

Present address: Life and Health Sciences, Pharmaceutical Sciences, Aston University, Aston Triangle, Birmingham B4 7ET. U.K.

[1] Abbreviations: U^P, 5-propargylamino-2′-dU; EA-T, 2′-aminoethoxy-T; bis-amino-U, 2′-aminoethoxy, 5-propargylamino-U.

10.1021/bi020164n CCC: $22.00
Published on Web 05/17/2002

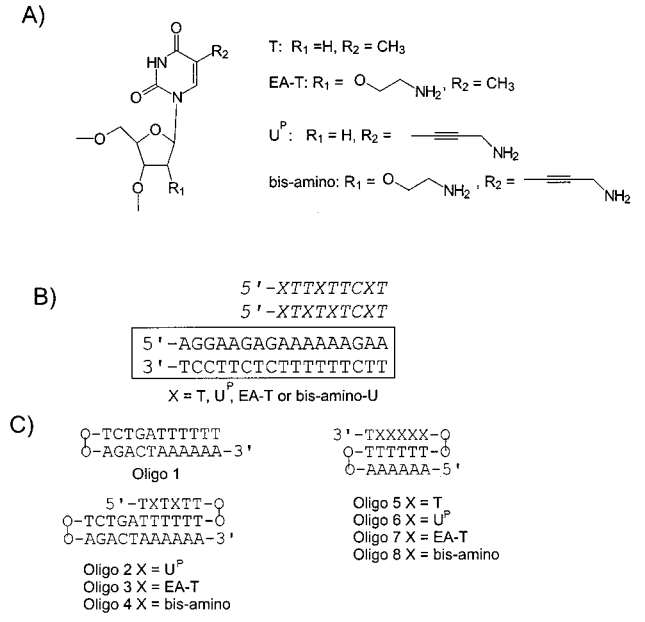

FIGURE 1: (A) Structures of thymine (T), 2′-aminoethoxy-T (EA-T), 5-propargylamino-dU (U^P), and bis-amino-U. (B) Sequence of the oligopurine tract (boxed), contained within the 110 base pairs fragment from *tyr*T(48−59). The third strand 9-mer oligonucleotides, used in the footprinting experiments, are shown above. (C) Oligonucleotides used to form intramolecular triplexes for use in UV-melting studies. The linkers between the strands were composed of two octanediol residues (O).

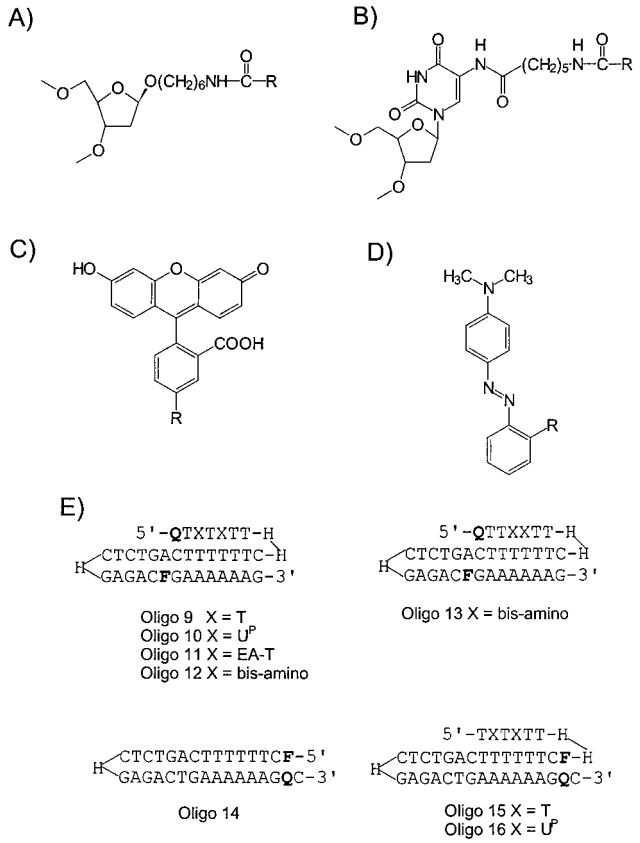

FIGURE 2: Chemical structures of (A) MeRd dR, R = methyl red and Fam dR, R = Fam; (B) FamCap-dU, R = Fam; (C) Fam; (D) methyl red. (E) Sequences of oligonucleotides used for the fluorescent melting studies with the Roche LightCycler. The different stands of these intramolecular complexes are joined by one or two hexaethylene glycol moieties (H). Q indicates the quencher, while F indicates the fluorophore. In each case, the quencher is MeRed dR. For oligonucleotides 9−13, the fluorophore is FamCap-dU, while this is Fam dR for oligonucleotides 14−16.

multiple substitutions with U^P form more stable complexes, and 9-mer oligonucleotides substituted in only three or four positions show only a small increase in triplex stability (*32*). Other groups have shown that addition of a positive charge at the 2′-position also greatly enhances triplex stability and demonstrated that the 2′-aminoethoxy group was the most efficient (EA-T, Figure 1A) (*35*−*39*).

We have recently prepared a nucleotide analogue containing both these substitutions (bis-amino-U, Figure 1A) (*40*). In this paper, we compare the stability of triplexes containing this analogue with those containing EA-T or U^P.

MATERIALS AND METHODS

Oligonucleotides. Oligonucleotides were synthesized on an Applied Biosystems 394 solid-phase DNA/RNA synthesizer on 1.0 μM scale, and were prepared and HPLC purified by Oswel Research Products Ltd., Southampton. Phosphoramidite monomers for the base modifications were prepared as previously described (*32*, *35*, *40*). Methyl red (Figure 2D) was incorporated at various positions in the oligonucleotides, using MeRed dR (Figure 2A). Fluorescein (Figure 2C) was incorporated using either Fam dR (Figure 2A) or FamCap-dU (Figure 2B). The sequences of oligonucleotides used in these studies are shown in Figures 1C and 2E.

*DNA Fragments. Tyr*T(43−59) is a modification of the original *tyr*T DNA sequence, which contains a 17-base oligopurine tract between positions 43−59 (*41*). The sequence of this region is shown in Figure 1B. The radiolabeled DNA fragment was prepared by digesting the plasmid with *Eco*RI and *Ava*I and was labeled at the 3′-end of the *Eco*RI site using reverse transcriptase and α-^{32}P-dATP. The labeled 110-base pair DNA fragment was separated from the remainder of the plasmid DNA on an 8% (w/v) nondenaturing polyacrylamide gel. The isolated DNA was dissolved in 10 mM Tris-HCl pH 7.5 containing 0.1 mM EDTA to give about 10−20 cps/μL as determined on a hand held Geiger counter (<10 nM). For quantitative footprinting experiments, the absolute DNA concentration is not important so long as it is lower than the dissociation constant of the DNA binding compound.

DNase I Footprinting. Radiolabeled DNA (1.5 μL) was mixed with oligonucleotides (1.5 μL) dissolved in an appropriate buffer. Experiments at pH 5.0 and 6.0 were performed in 50 mM sodium acetate containing 10 mM $MgCl_2$, while at pH 7.5 the buffer used was 10 mM Tris-HCl containing 50 mM NaCl and 10 mM $MgCl_2$. The concentrations refer to conditions in the final reaction mixture. These complexes were left to equilibrate at 20 °C for at least 2 h. The samples were digested by adding 2 μL of DNase I (typically, 0.01 Units mL^{-1}) dissolved in 20 mM NaCl containing 2 mM $MgCl_2$ and 2 mM $MnCl_2$. The reaction was stopped after 1 min by adding 5 μL of 80% formamide containing 10 mM EDTA, 10 mM NaOH, and 0.1% (w/v) bromophenol blue.

Gel Electrophoresis. The products of digestion were separated on 9% polyacrylamide gels containing 8 M urea. Samples were heated to 100 °C for 3 min, before rapidly cooling on ice and loading onto the gel. Polyacrylamide gels (40 cm long, 0.3 mm thick) were run at 1500 V for about 2

h and then fixed in 10% (v/v) acetic acid. These were transferred to Whatman 3MM paper and dried under vacuum at 80 °C. The dried gels were either exposed to autoradiography at −70 °C using an intensifying screen, or were subjected to phosphorimaging using a Molecular Dynamics STORM phosphorimager.

Quantitative Analysis. The intensity of bands within each footprint was estimated using ImageQuant software. These were normalized by comparison with a region for which DNase I cleavage was not affected. Footprinting plots (*42*) were constructed from these data and C_{50} values, indicating the oligonucleotide concentration, which reduces the band intensity by 50%, were calculated by fitting a simple binding curve to the data (*30*, *31*, *42*).

UV Melting. UV melting studies were performed as previously described (*43*) on a Perkin-Elmer Lambda 2 UV/Vis spectrometer with PTP-1 temperature programmer or Perkin-Elmer Lambda 15 UV/Vis specrometer. Absorbances were monitored at 260 nm. The heating rate was set at 1°/min, and absorbances were taken at intervals of 10 s. First derivatives were obtained using the Perkin-Elmer PECSS2 software. Each UV melting experiment was repeated until the three T_m values were within 0.5 °C. Experiments at pH 5.0−6.5 were performed in 50 mM sodium acetate buffer containing 100 mM NaCl. Between pH 7.0 and 8.0, the buffer used was 50 mM sodium phosphate containing 100 mM NaCl, while at pH 8.5−9.0 the buffer was 50 mM borate containing 100 mM NaCl. The oligonucleotide in the spectrophotometer cell was at a concentration of 3 μM. Sequences for the oligonucleotides used in these studies are shown in Figure 1C.

Fluorescence Melting. Fluorescence melting experiments were performed using the oligonucleotides shown in Figure 2E. Full details of this procedure are published elsewhere (*44*). Briefly, 20 μL of oligonucleotide (0.25 μM, diluted in the same buffers as used for the UV-melting studies) were placed in the Roche LightCycler glass capillary. Oligonucleotides were first denatured by heating to 95 °C for 5 min. They were then annealed by cooling to 25 °C at the slowest instrument rate (0.1°/s), held at 25 °C for 5 min and then melted by heating to 95 °C at 0.1°/s. Recordings were taken during both the annealing and denaturing steps and were found to be identical, indicating that system was at thermodynamic equilibrium. The LightCycler has one excitation source (488 nm); the changes in fluorescence emission were measured at 520 nm. T_m values were determined from the first derivatives of the melting profiles using the Roche LightCycler software. In some instances, the melting curves showed a small change in fluorescence with temperature in regions outside the melting transition; the data were not corrected for the temperature dependence of the fluorescence emission. Each reaction was performed in triplicate, and the T_m values usually differed by less than 0.5 °C.

RESULTS

DNase I Footprinting. We have previously shown that the oligonucleotide TTTTTTCTT binds only weakly to its 9-base pair target site, and fails to give a footprint, even at a concentration of 30 μM at pH 5.0 (*30*). The low affinity is thought to be due to the relatively weak stability of the T·AT triplet, compared with C^+·GC. This interaction has been stabilized by addition of triplex-binding ligands or by inclusion of modified bases. In particular, we have shown that replacement of seven of the Ts with propragylamino-dU (U^P) using the oligonucleotide $U^PU^PU^PU^PU^PU^PCU^PT$ increases the affinity by over 3 orders of magnitude, generating footprints at nanomolar concentrations (*32*). However, substitution of only four of the Ts required 20 μM oligonucleotide, while an oligonucleotide with only three substitutions failed to produce a clear footprint. We therefore examined the effect of substituting three or four of the Ts in this oligonucleotide with the new analogue 5-propargylamino,2′-aminoethoxy-U. For comparison, we prepared similar oligonucleotides substituted with 2′-aminoethoxy-T. The results of footprinting experiments with these oligonucleotides are shown in Figures 3 and 4. At pH 5.0, the oligonucleotide containing four 2′-aminoethoxy-T residues attenuates DNase I cleavage at the expected target site; this is accompanied by enhanced cleavage at the 3′- (lower) end of the target site, an effect that is often observed for triplex footprints. Quantitative analysis of this cleavage pattern generates the footprinting plot shown in Figure 5. Simple

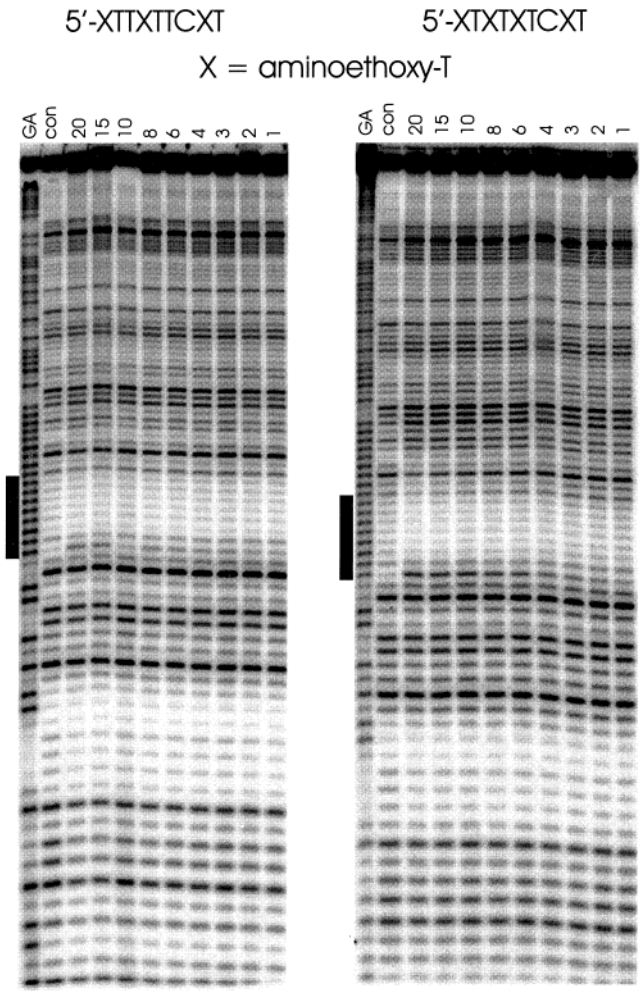

FIGURE 3: DNase I digestion patterns showing the interaction of aminoethoxy-U-substituted oligoncleotides with the oligopurine tract in *tyr*T(43−59). The experiments were performed in 50 mM sodium acetate buffer pH 5.0 containing 10 mM $MgCl_2$. Oligonucleotide concentrations (μM) are shown at the top of each gel lane. The tracks labeled "con" show DNase I digestion of the duplex DNA in the absence of oligonucleotide. "GA" represents Maxam−Gilbert markers specific for purines. The boxes show the position of the expected 9-mer target sites.

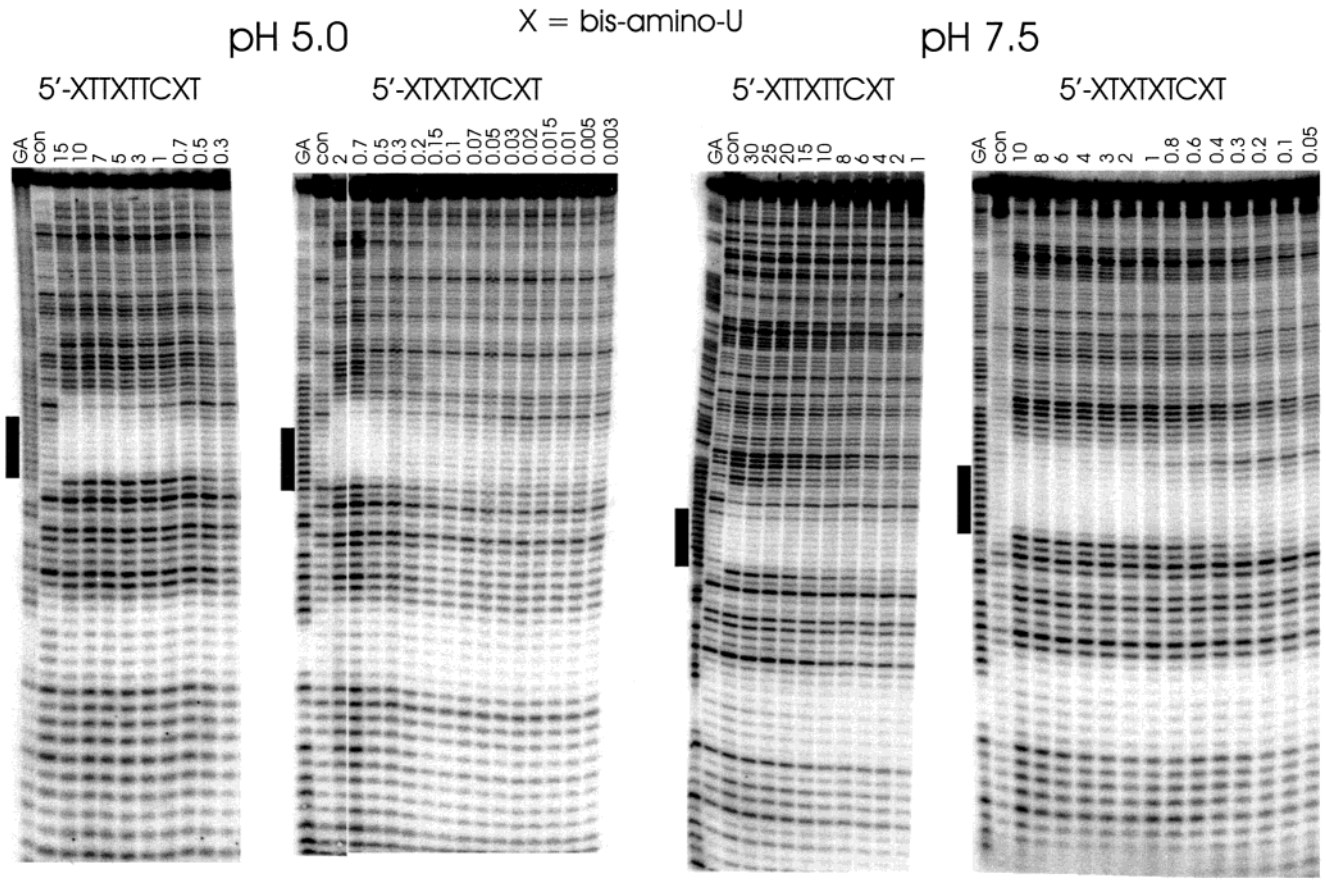

FIGURE 4: DNase I digestion patterns showing the interaction of bis-amino-U-substituted oligonucleotides with the oligopurine tract in *tyr*T(43−59). The experiments were performed in 50 mM sodium acetate buffer pH 5.0 containing 10 mM $MgCl_2$ or 10 mM Tris-HCl pH 7.5 containing 50 mM NaCl and 10 mM $MgCl_2$. Oligonucleotide concentrations (μM) are shown at the top of each gel lane. The tracks labeled "con" show DNase I digestion of the duplex DNA in the absence of oligonucleotide. "GA" represents Maxam−Gilbert markers specific for purines. The boxes show the position of the expected 9-mer target sites.

Table 1: C_{50} Values Derived from Footprinting Plots of the DNase I Cleavage Patterns in the Presence of the Different Oligonucleotides[a]

	XTTXTTCXT		XTXTXTCXT	
oligonucleotide	footprint C_{50} μM	enhancement C_{50} μM	footprint C_{50} μM	enhancement C_{50} μM
X = 5-propargylamino pH 5.0	NO	NO	21 ± 6	4.3 ± 0.9
X = 2′-aminoethoxy pH 5.0	NO	NO	6.9 ± 1.8	7.9 ± 1.2
X = bis-modified pH 5.0	0.83 ± 0.23	0.34 ± 0.16	0.13 ± 0.03	0.32 ± 0.20
X = bis-modified pH 7.5	23 ± 2	14 ± 5	0.54 ± 0.13	0.56 ± 0.16

[a] The data for 5-propargylamino-dU are taken from ref *31*. Note that the unmodified oligonucleotide 5′-TTTTTTCTT does not affect DNase I cleavage under any of these conditions. Similarly the mono-amino derivatives do not affect the DNase I cleavage pattern at pH 7.5. NO indicates no footprint detected with 30 μM oligonucleotide.

binding curves fitted to these data yield C_{50} values of 6.9 ± 1.8 and 7.9 ± 1.2 μM for the footprint and enhancement, respectively. In contrast, no footprint is evident for the oligonucleotide containing three 2′-aminoethoxy-dT residues. These C_{50} values are presented in Table 1, which also shows the values for 5-propargylamino-dU taken from previous work. The data show that each of these amino-modifications generates a similar effect on the binding affinity. No footprints were evident when these experiments were repeated at pH 7.5, as previously shown for oligonucleotides containing three or four 5′-propargylamino-dU residues.

The first two panels of Figure 4 show the results of similar experiments with oligonucleotides containing three or four bis-amino modified bases, performed at pH 5.0. It can be seen that both oligonucleotides generate clear footprints at the target site, which are accompanied by enhanced cleavage at the 3′-end. Quantitative analysis of these footprints and enhancements produces the footprinting plots shown in Figure 5. The C_{50} values estimated from these data are shown in Table 1. It is clear that the oligonucleotide containing only three modifications binds with appreciable affinity. Similar experiments were also performed at pH 7.5, and are shown in the final two panels of Figure 4. Even under these conditions, in which the degree of cytosine protonation is much reduced, both oligonucleotides produce DNase I footprints. The footprinting plots are shown in Figure 5, and the C_{50} values are presented in Table 1. It can be seen that there is little decrease in affinity for the four-substituted oligonucleotide between the two pHs. It is clear that that the bis-amino derivative produces a large increase in triplex stability which is much greater than that generated by either substitution alone.

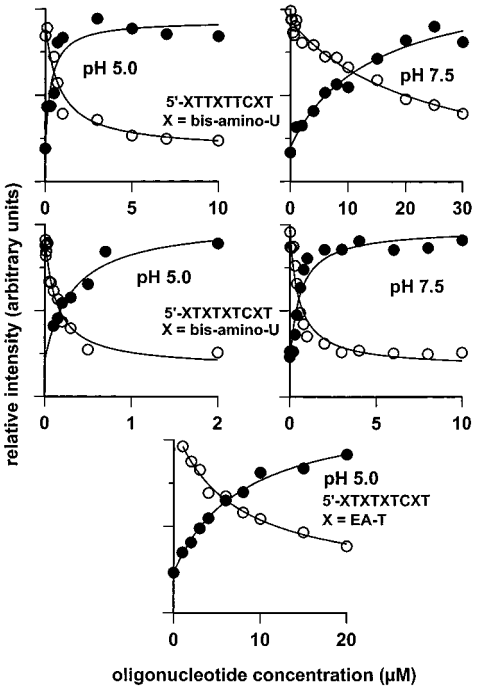

FIGURE 5: Footprinting plots showing the interaction of oligonucleotides with the target site in *tyr*T(43−59). The data were taken from quantitative analysis of the gels presented in Figures 2 and 3. In each case, the abscissa shows the oligonucleotide concentration (μM), while the ordinate shows the relative intensity of bands in the footprint, plotted on an arbitrary scale. The curves fitted to the data are simple binding curves corresponding to the C_{50} values shown in Table 1. In each case, the open circles correspond to the reduction in intensity seen at the footprinting site, while the filled circles correspond to the enhanced cleavage observed at the triple-duplex junction.

UV Melting Studies. UV-melting curves were determined for oligos 5−8 (Figure 1C) containing the sequences A_6−T_6−X_5T. These oligonucleotides generate short intramolecular triplexes in which the three strands are covalently linked by octanediol residues. We have shown that at pH 7.0 (50 mM sodium phosphate buffer, containing 100 mM NaCl) oligonucleotides in which X = T or U^P melt with a single transition at 314 and 335.5 K, respectively (*32*). When X was replaced with aminoethoxy-T or bis-amino-U, this again yielded single melting transitions at 332.5 and 336.8 K, respectively. These results demonstrate that both analogues stabilize this intramolecular triplex and suggest that the rank order of stabilization might be aminoethoxy-T < propragylamino-dU < bis-amino-U. However, we were concerned that the more stable duplex-single strand might affect or mask the triplex−duplex melting transition. We therefore designed further oligonucleotides in which the duplex is seven base pairs longer than the triplex (oligos 2−4) in an attempt to separate the duplex and triplex melting transitions. Representative melting curves for these oligonucleotides are shown in Figure 6 and the full range of data are summarized in Table 2. So as not to stabilize the triplex too far, only two out of the six thymines were substituted with the base analogues. The data for the unmodified and U^P-containing oligonucleotides have been previously presented (*30*, *32*). As expected oligo 1, corresponding to the duplex, melted with a single transition at all pHs with T_m values of around 335 K. Oligo 2 (corresponding to P2 in our previous work (*32*)) displayed two melting transitions, corresponding to

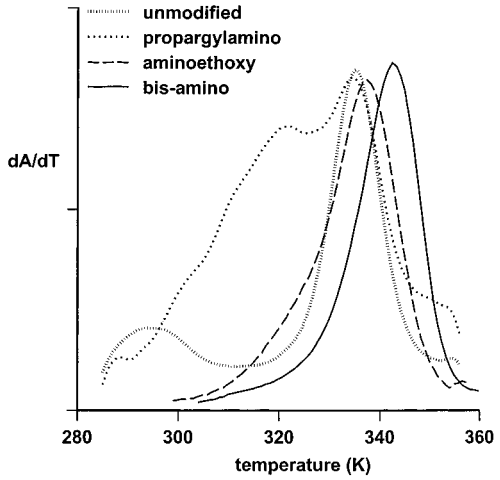

FIGURE 6: UV-melting profiles for intramolecular triplexes, measured at pH 7.0. The ordinate shows the first differential of the melting curves (d*A*/d*T*). The data for the unmodified triplex and for propargylamino-dU were taken from ref *32*.

Table 2: T_m Values for the Different Oligonucleotides Determined from UV-melting Studies

	T_m (K)			
pH	oligo 1	oligo 2	oligo 3	oligo 4
5.0	334.9	326.8	335.3	343.0
6.0	335.9	323.6	337.0	343.9
7.0	334.5	320.8	337.5	343.7
8.0	335.2	314.7	338.2	340.1
9.0			335.0	335.0

triplex−duplex and duplex-single strands. The lower transition moved to lower temperatures at elevated pHs presumably due to partial deprotonation of the propargylamino side group. In contrast, the complexes containing two aminoethoxy-T or bis-amino-U residues showed only a single melting transition under all conditions. The T_m values for oligo 3 are fairly constant across all the pHs, whereas oligo 4 shows a decrease in stability above pH 8.0, though this is less pronounced than with oligo 2. At low pHs, the bis-substituted oligonucleotide is 8 K more stable than the oligonucleotide substituted with only aminoethoxy-T, and melts at temperatures above that of the underlying duplex (oligo 1). These results therefore confirm that bis-amino-U produces a marked increase in triplex stability which is greater than that produced by either the 5′-propargylamino or 2′-aminoethoxy substitution alone.

Fluorescence Melting Curves. Although the UV-melting results presented above confirm that the bis-amino-U substitution enhances triplex stability, it is difficult or impossible to distinguish between the triplex−duplex and duplex−single strand transitions. We have therefore devised a novel fluorescence-based method, the full details of which presented elsewhere have been (*44*), which allows us to observe these two transitions independently. The oligonucleotides used for this work are presented in Figure 2E and each contain a fluorophore (F, fluorescein) and quencher (Q, methyl red) positioned so that they are in close proximity, and the fluorescence is quenched when the oligonucleotide folds into an intramolecular triplex. When the oligonucleotide melts these two groups are separated, and there is a large increase in fluorescence. Oligonucleotides 9−12 are designed with the fluorophore and quencher in third strand and duplex

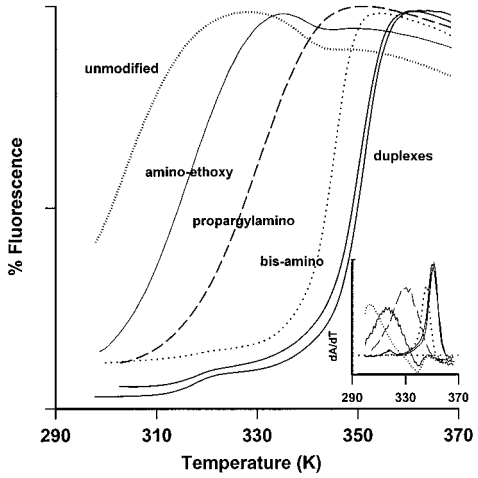

FIGURE 7: Fluorescence-melting curves for oligonucleotides which form intramolecular complexes, measured at pH 7.0. In each case, the oligonucleotide concentration was 0.25 μM unmodified, propargylamino, aminoethoxy, and bis-amino correspond to oligos 9−12, respectively. The ordinate represents the relative fluorescence of each oligonucleotide as a function of temperature. The duplexes correspond to oligos 14 (right-hand curve) and 16. The inset shows first differentials of these data.

purine strand, respectively, so that the increase in fluorescence will represent dissociation of the triplex. In contrast, oligos 15 and 16 form the same intramolecular triplexes, but the fluorophore and quencher are positioned in either strand of the duplex, so that the fluorescence increase represents melting of the duplex only. Oligo 14 only contains the duplex found in the other triplexes. Melting experiments with these oligonucleotides were performed in parallel using the Roche LightCycler. Representative examples are shown in Figure 7, and the T_m values are summarized in Table 3. Considering first the unmodified triplex (oligo 9), this melts with a T_m between 301 and 309 K. In contrast, the duplex melt for this intramolecular triplex is seen with oligo 15 and is about 350 K. This is very similar to the values obtained for the duplex alone (oligo 14). Oligos 10−12 show the effect of substituting two of the third strand Ts with the three different base analogues. All three triplexes melt at much higher temperatures than the unmodified complex. In general, the complexes with propargylamino-dU are more stable than those with 2′-aminoethoxy-T. The bis-amino-U modification produces the most stable complexes, which melt at temperatures similar to that of the underlying duplex, confirming the cooperative nature of this melting process. As expected, oligos 10 and 11 show pH-dependent melting profiles, becoming less stable at elevated pHs, with 9.1 and 6.5 K decreases between pH 5.0 and 8.0, respectively. Although bis-amino-U also shows a pH-dependent decrease in T_m this is less pronounced, with only a 4.0 K decrease over the same pH range. Interestingly, oligo 13, in which the two modified bases are placed adjacent to each other, shows nearly identical melting properties to oligo 12 in which they are separated by one base.

DISCUSSION

The data presented in this paper clearly demonstrate that dU bases containing both 2′-aminoethoxy and 5′-propargylamino substituents form much more stable triplexes than those containing either substitution alone. This stabilization is observed with both intermolecular (footprinting) and intramolecular (UV and fluorescence melting) complexes. The fluorescence melting experiments show that 5-propargylamino and 2′-aminoethoxy substituents have an additive effect in the bis-substituted derivative. The data at pH 7.0 (Table 3) show that U^P or EA-T modifications produce ΔT_m values of 27.1 and 12.5 K, respectively. This compares with 42.4 K for the bis-amino derivative, which is slightly greater than the sum of the other two. The additive effect of the two substitutions suggests that these groups are contacting different phosphates. It is also noteworthy that the bis-modified derivative is less pH dependent than the other derivatives though, as expected, the stability decreases above pH 8.0, consistent with amino-phosphate interactions.

The footprinting studies show that a 9-mer oligonucleotide containing four bis-amino-U residues forms a complex with submicromolar affinity even at pH 7.5, despite the fact that this contains a single C·GC triplet. This is therefore one of the strongest parallel triplexes reported so far.

To explain the stabilization produced with bis-amino derivative, we have performed some simple modeling studies. A section of the resulting structure is shown in Figure 8. This model was derived by manually adding a 5-propargylamino group to the NMR structure of the EA-T containing triplex, which has previously been reported (*37*, *38*). No energy minimization was performed. A section of this model is presented in Figure 8, showing the U^P-A Hoogsteen pair, together with the third strand T on the 5′-side of U^P. As previously reported (*37*, *38*), the 2′-aminoethoxy group makes a specific contact with a phosphate on the purine strand of the duplex, with an N−O distance of about 2.8 Å. The amino group of the propargylamino substituent is able to interact with its own 5′-phosphate with an N−O distance of 3.0 Å. In addition, there is a possible hydrophobic contact between the propyne moiety and the 5-methyl group of the adjacent third strand base (2.4 Å). The propargylamino group is also 4.7 Å from the next third strand phosphate group. On rotating by 50° about the propyne CH_2 group, both N−O phosphate distances become 4.2 Å, though this is too large for a strong ion-pair interaction. Both contacts may be possible if minor changes occur in the structure of the

Table 3: T_m Values for Various Oligonucleotides Determined by Fluorescence Melting Studies[a]

	T_m (K)							
pH	oligo 9	oligo 10	oligo 11	oligo 12	oligo 13	oligo 14	oligo 15	oligo 16
5.0	308.6	333.5	321.0	346.9	346.5	348.3	348.1	348.2
6.0	303.6	331.2	317.5	346.7	346.0	351.0	349.9	350.5
7.0	303.3	330.4	315.8	345.7	345.2	351.3	351.1	350.4
8.0	303.4	324.4	314.5	342.9	342.7	351.3	351.1	350.5
9.0	301.0	307.5	304.7	325.5	325.3	347.6	347.2	346.5

[a] The oligonucleotide concentration was 0.25 μM in each case.

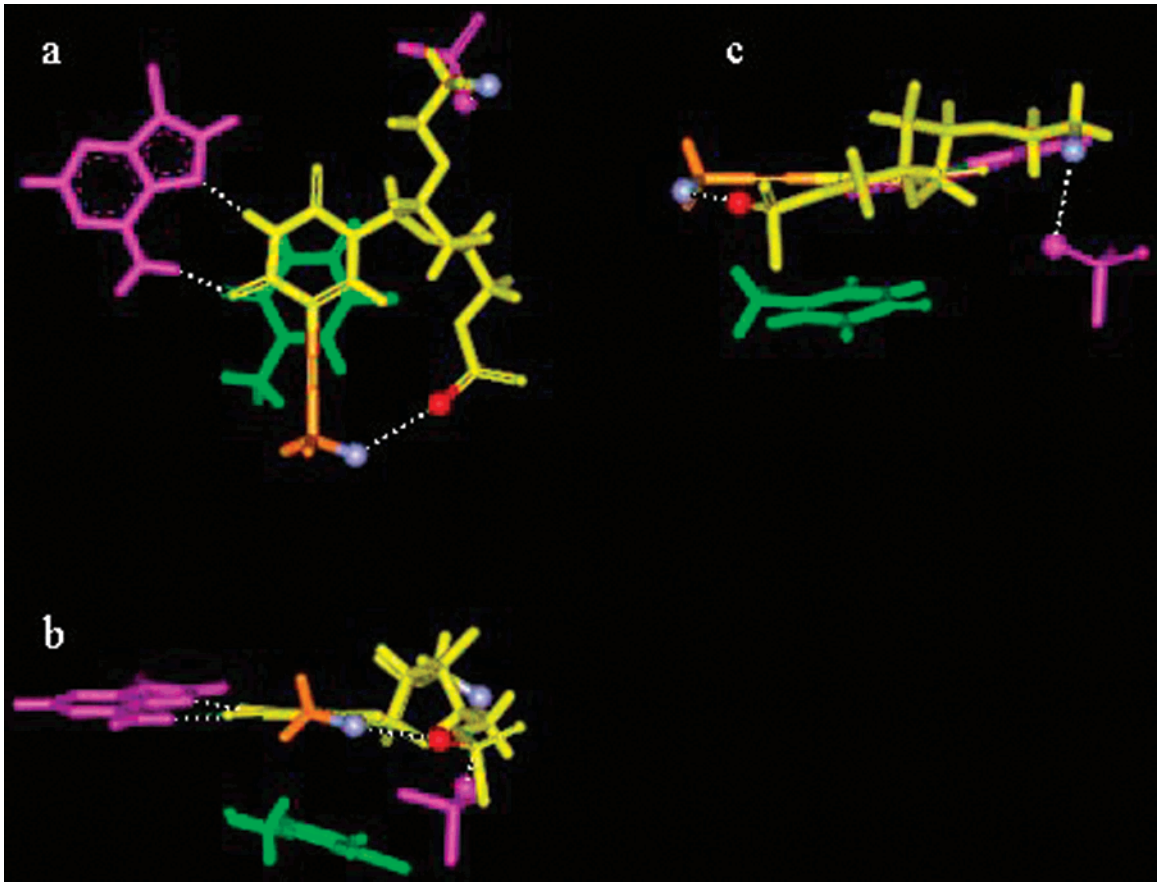

FIGURE 8: Models showing possible interactions formed with the bis-amino derivative. (a) A top view looking down the helix axis, while (b) and (c) are side views. For each view, the bis-amino-dU residue is shown in yellow with its propargylamino group in orange. The amino group is shown as a blue sphere interacting with its own 5′-phosphate group (oxygen in red). The amino group from the 2′-aminoethoxy moiety is also shown as a blue sphere interacting with a phosphate from the purine strand of the duplex (in purple). The adenosine which is Hoogsteen bonded to the bis-amino-U is shown in purple. The T on the 5′-side of U^p is shown in green. Putative hydrogen bonds and ion-pairs are shown as white dotted lines.

underlying DNA. However, a definite model will require high-resolution NMR or X-ray data. The interaction of the 5′-propargylamino group with phosphate on the same strand suggests that this substituent may restrict the rotational freedom of the third strand and help to preorganize it ready for triplex formation.

It is worth noting that, even though the stabilization arises from charge effects, the third strand oligonucleotides form specific complexes and their sequence recognition properties are not obviously affected. This is apparent with the footprinting data for which the footprints are found in the predicted positions, and there are no other changes in the cleavage pattern in the remainder of the 100 base pair fragment.

In contrast to C^+·GC triplets, adjacent bis-amino-U-containing triplets do not appear to be destabilizing. This emphasizes the importance of removing the positive charge from the bases and placing it on a substituent that is able to neutralize the negatively charged phosphodiester backbone. Since each base triplet is connected to three phosphates, the X·AT triplets formed with this analogue will still have an overall net negative charge. This strategy of appending positively charged moieties to the DNA bases at specific loci should be generally applicable to the triplex strategy, and we are extending it to other bases. The addition of 2′-aminoethoxy to C has been previously shown to stabilize the C^+·GC triplet (*35*, *37*), though in this instance addition of a 5′-propargylamino group will not be beneficial as it will decrease the pK_a of the N(3) atom of cytosine. This base analogue will therefore be unable to form two hydrogen bonds to the GC base pair.

REFERENCES

1. Soyfer, V. N., and Potoman, V. N. (1996) *Triple-Helical Nucleic Acids*, Springer-Verlag, New York.
2. Thuong, N. T., and Hélène, C. (1993) Sequence specific recognition and modification of double helical DNA by oligonucleotides. *Angew. Chem., Int. Ed. Engl. 32*, 666−690.
3. Neidle, S. (1997) Recent developments in triple helix regulation of gene expression. *Anti-Cancer Drug Des. 12*, 433−442.
4. Vasquez, K. M., and Wilson, J. H. (1998) Triplex-directed modification of genes and gene activity. *Trends Biochem Sci. 23*, 4−9.
5. Chan, P. P., and Glazer, P. M. (1997) Triplex DNA: fundamental advances and potential applications for gene therapy. *J. Mol. Med. 75*, 267−282.
6. Praseuth, D., Guieysse, A. L., and Hélène, C. (1999) Triple helix formation and the antigene strategy for sequence-specific control of gene expression. *Biochim. Biophys. Acta 1489*, 181−206.
7. Knauert, M. P., and Glazer, P. M. (2001) Triplex forming oligonucleotides: sequence-specific tools for gene targeting. *Mol. Hum Genet. 20*, 2243−2251.
8. Majumdar, A., Khorlin, A., Dyatkina, N., Lin, F. L. M., Powell, J., Liu, J., Feiz, Z. Z., Khripine, Y., Watanabe, K. A., George, J., and Glazer, P. M. (1998) Targeted gene knockout mediated by triple helix forming oligonucleotides. *Nat. Genet. 20*, 212−214.

9. Fox, K. R. (2000) Targeting DNA with triplexes. *Curr. Med. Chem. 7*, 17−37.
10. Moser, H. E., and Dervan, P. B. (1987) Sequence-specific cleavage of double-helical DNA by triple helix formation. *Science 238*, 645−650.
11. Beal, P. A., and Dervan, P. B. (1991) Second structural motif for recognition of DNA by oligonucleotide-directed triple-helix formation. *Science 251*, 1360−1363.
12. Gowers, D. M., and Fox, K. R. (1999) Towards mixed sequence recognition by triple helix formation. *Nucleic Acids Res. 27*, 1569−1577.
13. Mergny, J. L., Duval-Valentin, G., Nguyen, C. H., Perrouault, L., Faucon, B., Rougée, M., Montenay-Garestier, T., Nisagni, E., and Hélène, C. (1992) Triple-helix specific ligands. *Science 256*, 1681−1684.
14. Escudé, C., Garestier, T., and Sun, J.-S. (2000) Drug interaction with triple-helical nucleic acids. *Methods Enzymol. 340*, 340−357.
15. Kukreti, S., Sun, J. S.; Garestier, T., and Hélène, C. (1997) Extension of the range of DNA sequences available for triple helix formation: stabilization of mismatched triplexes by acridine-containing oligonucleotides. *Nucleic Acids Res. 25*, 4264−4270.
16. Zhou, B. W., Puga, E., Sun, J. S., Garestier, T., and Hélène, C. (1995) Stable triple helices formed by acridine-containing oligonucleotides with oligopurine tracts of DNA interrupted by one or two pyrimidines. *J. Am. Chem. Soc. 117*, 10425−10428.
17. Sun, J.-S., Francois, J.-C., Montenay-Garestier, T., Saison-Behmoaras, T., Roig, V., Thuong, N. T., and Hélène, C. (1989) Sequence specific intercalating agents: Intercalation at specific sequences on duplex DNA via major groove recognition by oligonucleotide-intercalator conjugates. *Proc. Natl. Acad. Sci. U.S.A. 86*, 9198−9202.
18. Tung, C.-H., Breslauer, K. J., and Stein, S. (1993). Polyamine-linked oligonucleotides for DNA triple helix formation. *Nucleic Acids Res. 21*, 5489−5494.
19. Sund, C., Puri, N., and Chattopadhyaya, J. (1997). The chemistry of *C*-branched spermine tethered oligo-DNAs and their properties in forming duplexes and triplexes. *Nucleosides Nucleotides 16*, 755−760.
20. Barawkar, D. A., Rajeev, K. G., Kumar, V. A., and Ganesh, K. N. (1996). Triplex formation at physiological pH by 5-MedC-N4-(spermine) [X] oligonucleotide. *Nucleic Acids Res. 24*, 1229−1237.
21. Nara, H., and Ono, A. (1995). DNA duplex and triplex formation and resistance to nucleolytic degradation of oligodeoxynucleotides containing *syn* nor-spermine at the 5′-position of 2′deoxyuridine. *Bioconjug. Chem. 6*, 54−61.
22. Lacroix, L., Arimondo P. B., Takasugi, M., Hélène, C., and Mergny, J. L. (2000) Pyrimidine morpholino oligonucleotides form a stable triple helix in the absence of magnesium ions. *Biochem. Biophys. Res. Commun. 270*, 363−369.
23. Gryaznov, S. M. (1999) Oligonucleotide N3 ′→P5 ′ phosphoramidates as potential therapeutic agents. *Biochim. Biophys. Acta 1489*, 131−140.
24. Vasquez, K. M., Dagle, J. M., Weeks, D. L., and Glazer, P. M. (2001) Chromosome targeting at short polypurine sites by cationic triplex-forming oligonucleotides. *J. Biol. Chem. 276*, 38536−38541.
25. Godde, F., Toulmé, J. J., and Moreau, S. (1998) Benzoquinazoline derivatives as substitutes for thymine in nucleic acid complexes. Use of fluorescence emission of benzo[*g*]-quinazoline-2, 4-(1*H*, 3*H*)-dione in probing duplex and triplex formation. *Biochemistry 37*, 13765−13775.
26. Michel, J., Toulmé, J. J., Vercauteren, J., and Moreau, S. (1996) Quinazoline-2, 4(1*H*, 3*H*)-dione as a substitute for thymine in triple-helix forming oligonucleotides: A reassessment. *Nucleic Acids Res. 24*, 1127−1135.
27. Staubli, A. B., and Dervan, P. B. (1994) Sequence specificity of the nonnatural pyrido[2, 3-*d*]pyrimidine nucleoside in triple helix formation. *Nucleic Acids Res. 22*, 2637−2642.
28. Asensio, J. L., Lane, A. N., Dhesi, J., Bergqvist, S., and Brown, T. (1998) The contribution of cytosine protonation to the stability of parallel DNA triple helices. *J. Mol. Biol. 275*, 811−822.
29. Völker, J., and Klump, H. H. (1994) Electrostatic effects in DNA triple helices. *Biochemistry 33*, 13502−13508.
30. Keppler, M. D., and Fox, K. R. (1997) Relative stability of triplexes containing different numbers of T·AT and C^+·GC triplets. *Nucleic Acids Res. 25*, 4644−4649.
31. Gowers, D. M., Bijapur, J., Brown, T., and Fox, K. R. (1999) DNA triple helix formation at target sites containing several pyrimidine interruptions: Stabilization by protonated cytosine or 5-(1-propargylamino)dU. *Biochemistry 38*, 13747−13758.
32. Bijapur, J., Keppler, M. D., Bergqvist, S., Brown, T., and Fox, K. R. (1999) 5-(1-propargylamino)-2′-deoxyuridine (U^P): a novel thymidine analogue for generating DNA triplexes with increased stability. *Nucleic Acids Res. 27*, 1802−1809.
33. Colocci, N., and Dervan, P. B. (1994). Cooperative binding of 8-mer oligonucleotides containing 5-(1-propynyl)-2′-deoxyuridine to adjacent DNA sites by triple helix formation. *J. Am. Chem. Soc. 116*, 785−786.
34. Phipps, K. A., Tarköy, M., Schultze, P., and Feigon, J. (1998) Solution structure of an intramolecular DNA triplex containing 5-(1-propynyl)-2′-deoxyuridine residues in the third strand. *Biochemistry 37*, 5820−5830.
35. Cuenoud, B., Casset, F., Hüsken, D., Natt, F., Wolf, R. M., Altmann, K.-H., Martin, P., and Moser, H. E. (1998) Dual recognition of double-stranded DNA by 2′-aminoethoxy-modified oligonucleotides. *Angew. Chem., Int. Ed. 37*, 1288−1291.
36. Puri, N., Majumdar, A., Cuenoud, B., Natt, F., Martin, P., Boyd, A. Miller, P. S., and Seidman, M. M. (2001) Targeted gene knockout by 2′-*O*-aminoethyl modified triplex forming oligonucleotides. *J. Biol. Chem. 276*, 28991−28998.
37. Blommers, M. J. J., Natt, F., Jahnke, W., and Cuenoud, B. (1998) Dual recognition of double-stranded DNA by 2′-aminoethoxy-modified oligonucleotides: The solution structure of an intramolecular triplex obtained by NMR spectroscopy. *Biochemistry 37*, 17714−17725.
38. Carlomagno, T., Blommers, M. J. J., Meiler, J., Cuenoud, B., and Griesinger, C. (2001) Determination of aliphatic side-chain conformation using cross-correlated relaxation: Application to an extraordinarily stable 2′-aminoethoxy-modified oligonucleotide triplex. *J. Am. Chem. Soc. 123*, 7364−7370.
39. Stütz, A. M., Hoeck, J., Natt, F., Cuenoud, B., and Woisetschläger, M. (2001) Inhibition of interleukin-4 and CD40-induced IgE germline gene promoter activity by 2′-aminoethoxy-modified triplex-forming oligonucleotides. *J. Biol. Chem. 276*, 11759−11765.
40. Sollogoub, M., Dominguez, B., Fox, K. R., and Brown, T. (2000) Synthesis of a novel bis-amino-modified thymidine monomer for use in DNA triplex stabilisation. *Chem. Commun. 2000*, 2315−2316.
41. Brown, P. M., Madden, C. A., and Fox, K. R. (1998) Triple helix formation at different positions on nucleosomal DNA. *Biochemistry 37*, 16139−16151.
42. Dabrowiak, J. C., and Goodisman, J. (1989) Quantitative footprinting analysis of drug−DNA interactions. In *Chemistry and Physics of DNA-Ligand Interactions* (Kallenbach, N. R., Ed.) pp 143−174, Adenine Press, New York.
43. Ebel, S., Lane, A. N., and Brown, T. (1992) Very stable mismatch duplexes − structural and thermodynamic studies on tandem G. A mismatches in DNA. *Biochemistry 31*, 12083−12086.
44. Darby, R. A. J., Sollogoub, M., McKeen, C., Brown, L., Risitano, A., Brown, N., Barton, C., Brown, T., and Fox, K. R. (2002) High throughput measurement of duplex, triplex, and quadruplex melting curves using molecular beacons and the LightCycler. *Nucleic Acids Res. 30 (9)*, e39.

BI020164N